

# Temperature oscillation of a dual compensation chamber loop heat pipe under acceleration conditions

Xiaochen Lv<sup>a</sup>, Yongqi Xie<sup>b,\*</sup>, Hongxing Zhang<sup>c</sup>, Yanmeng Xu<sup>d</sup>, Hongwei Wu<sup>e,\*\*</sup>, Rodney Day<sup>e</sup>, Jianwei Ren<sup>f</sup>

<sup>a</sup>Qian xuesen laboratory of Space Technology, China Academy of Space Technology, Beijing 100094, China

<sup>b</sup>School of Aeronautic Science and Engineering, Beihang University, Beijing, 100191, China

<sup>c</sup>Beijing Key Laboratory of Space Thermal Control Technology, China Academy of Space Technology, Beijing 100094, China

<sup>d</sup>Cleaner Electronics Group, College of Engineering, Design and Physical Sciences, Brunel University, Uxbridge, UK

<sup>e</sup>School of Physics, Engineering and Computer Science, University of Hertfordshire, AL10 9AB, UK

<sup>f</sup>Department of Mechanical Engineering Science, University of Johannesburg, Cnr Kingsway and University Roads, Auckland Park, 2092, Johannesburg, South Africa

\*Corresponding Author (Dr. Yongqi Xie): Email: [xyq@buaa.edu.cn](mailto:xyq@buaa.edu.cn) Tel: +86(10)82338081

\*\*Corresponding Author (Dr. Hongwei Wu): Email: [h.wu6@herts.ac.uk](mailto:h.wu6@herts.ac.uk) Tel: +44(0)1707284265

## ABSTRACT

Loop heat pipe has a wide application in the fields of airborne electronics cooling and thermal management. However, the pertinent temperature oscillation of the loop heat pipe could lead to adverse effects on the electronics. In the current study, an ammonia-stainless steel dual compensation chamber loop heat pipe was developed to experimentally investigate the temperature oscillation under different acceleration conditions. The impact of several control parameters such as different heat loads, loading modes, acceleration directions and magnitudes on the operational performance of the loop heat pipe was analyzed in a systematic manner. The heat load applied on the evaporator ranged from 25 W to 300 W. The acceleration magnitude varied from 1g to 9g and four different acceleration direction, i.e. configurations A, B, C and D, were taken into account. Two different loading modes were applied with different heat load and acceleration force. Experimental results show that (i) the loop temperature will change and oscillate as the acceleration force was applied under all test conditions. It can be easily found that the temperature oscillation occurred at both heat loads of 250 W and 300 W. (ii) for the case of the first loading mode, periodic temperature oscillation is observed on the liquid line, whereas for the second loading mode, periodic temperature oscillation can be easily appeared on the entire loop. (iii) the loop temperature under both configurations A and B with acceleration of 7g does not oscillate at heat load of 150 W, 200 W and 250 W when the first loading mode is applied. Especially under configuration B, the acceleration could contribute to repress the temperature oscillation. Under the current heat loads for almost all cases, the temperature oscillation can be observed for configurations A, C and D with acceleration of 5g. (iv) the amplitude of evaporator at heat load of 300 W under configuration C are 0.6 °C, 0.3 °C, 0.2 °C and 0.3 °C with acceleration of 3g, 5g, 7g and 9g. The corresponding period is 66 s, 36 s, 34 s and 36 s, respectively.

**KEY WORDS:** Electronic cooling, loop heat pipe, dual compensation chamber, operating characteristics, elevated acceleration, temperature oscillation.

## 1. INTRODUCTION

With the vigorous development of minimized electronic equipment and increased power density, effective cooling of electronic equipment is facing severe challenges. Among the advanced cooling

technologies [1-3], loop heat pipes (LHPs) is considered as one of the most efficient cooling systems to achieve high heat transfer performance compared with some active thermal control components. It is recognized that LHPs have been widely used in the ground and aeronautic applications [4-6] due to its advantages such as no moving part, no extra energy consumption, long distance heat transport and high space layout flexibility.

Over the past two decades, extensive studies on the LHP for various applications have been conducted and it is identified that the temperature oscillation would occur under some conditions. This could deteriorate the temperature control performance and further lead to the damage of the electronic components. Goncharov et al. [7] experimentally investigated the temperature fluctuations of three different types of LHPs. They found two types of temperature fluctuations such as high frequency and low frequency fluctuations and provided possible explanations for the initiation and termination of such fluctuation. Ku et al. [8] conducted experimental study on temperature oscillation of a miniature LHP by changing the heat load and the sink temperature under terrestrial conditions. It was revealed that the reason was the thermal and hydrodynamic interactions between the evaporator, the compensation chamber (CC) and the condenser. Later on, Ku et al. [9, 10] also experimentally investigated the transient performance of a propylene LHP with a large thermal mass attached to the evaporator. Two types of temperature oscillation such as low frequency/high amplitude [9] and high frequency/low amplitude [10] were comprehensively analyzed. It was found that a constant evaporator power coupled with an oscillatory sink temperature and a constant sink temperature coupled with an oscillatory evaporator power could result in low frequency/high amplitude temperature oscillation. The effect of the sink temperature, evaporator power, fluid inventory, thermal conductance between thermal mass and evaporator as well as the heat leak from the evaporator to the CC were evaluated on the temperature oscillation [9]. On the other hand, the fast movement of the vapor front in the condenser was the source of high frequency/low amplitude temperature oscillation. Generally, the amplitude of the temperature oscillation was the largest of the liquid line but the smallest of the CC. The influence factor included the evaporator power, body forces, sink temperature, pressure drop in the loop, the loop orientation and active control of the CC temperature [10]. Chen et al. [11] experimentally investigated the transient performance of an ammonia-stainless steel miniature LHP at four vertical orientations and reached the same conclusions as Ku et al. [10]. They also considered that the vapor bubbles appearing in the liquid line initiated the oscillation. Temperature oscillations significantly depended on the orientation of the LHP.

Based on the mass, energy and momentum conservation laws, Launary et al. [12] developed a transient model to predict the whole LHP dynamic performance. Their model could be used to simulate the above two types of oscillation: high frequency/ low amplitude and low frequency/high amplitude temperature oscillations. Hoang and Baldauff [13] proposed the concept of stability of a nonlinear dynamical system for a LHP. They stated that the temperature oscillation depended on the proper combination of LHP components and the operating conditions. Stability criterion showed that high vapor generation in the CC could make the LHP to be less stable. The study on the temperature oscillation of a water-copper miniature LHP with flat evaporator was experimentally performed by Zhang et al. [14]. It was proposed that the insufficient capillary force and phase distribution of the working fluid were the two main reasons leading to the unstable operation of the LHP. Lin et al. [15, 16] performed a series of experimental investigations on the operating instability for an ammonia-stainless steel dual compensation chamber LHP (DCCLHP). It was found that the temperature fluctuation occurred during the operating period. It preferred to happen at low heat load of 5 W startup or at high heat load of 250 W-300 W during steady-state operation, especially under the orientation of the CC with bayonet through above the evaporator. However, the detailed analysis on the unstable phenomenon was not presented. Adachi et al. [17] developed a transient model to understand the internal flow as temperature oscillation occurred. They found that the two-phase flow inside the liquid line could result in the temperature oscillation. The higher the amplitude of the condensation length, the higher the temperature amplitude. According to the visualization study, Zhang et al. [18] proved that the temperature oscillations in the LHP were related to the fluctuations of both the vapor-liquid interface and pressure in the evaporator-CC coupling structure. Gai [19] believed that the instability

of the vapor-liquid two-phase flow could lead to the temperature oscillation of LHP by experimental and theoretical study. Li et al. [20] designed and tested two types of LHPs and it was found that the usage of the pressure head of evaporation was conducive to suppress the temperature oscillation during the LHP operation, especially at high heat load condition. He et al. [21] experimentally observed that the temperature oscillations at the condenser inlet could possess the large amplitude, further leading to other characteristic point fluctuations. One way increasing the heat sink temperature is proposed to eliminate the oscillations. By comparing the performance of three types of LHPs with single-layer wick of different pore sizes, Xu et al. [22] found a periodic temperature oscillations. Due to the relatively lower flow rate in the wick of small pore size, the temperature oscillation was only observed when the LHP started initially. When the steady states were achieved, the periodic temperature oscillation diminished and almost vanished.

The above studies in terrestrial gravity indicated that the thermal and hydrodynamic equilibrium destruction and vapor-liquid phases redistribution are the fundamental reason of temperature oscillation. However, when the LHPs are used to cool the electronic devices on the advanced military aircrafts which always suffer acceleration force with various magnitudes and directions. The acceleration force will be more likely to cause the equilibrium destruction and vapor-liquid distribution change in the loop. The loop temperature oscillation could normally be observed under this condition. It is recognized that there are only several literatures reporting the temperature oscillation of the LHP under acceleration fields. Ku et al. [8] also discussed the temperature oscillation of the LHP under periodic acceleration conditions. Their results showed that the change of the flow distribution among LHP components was definitely caused by the acceleration force, which could lead to the temperature oscillation to occur or to disappear. Afterwards, they [23] further experimentally studied the effect of the acceleration force on the operating performance of a miniature LHP. The acceleration ranged from 1.2g to 4.8g. They found that the temperature oscillations were observed in almost every test. The acceleration force could increase or decrease the oscillatory magnitude and even produced or eliminated the oscillation without variation of sink temperature or heat load. Fleming et al. [24] experimentally examined the performance of a titanium-water LHP in standard and elevated acceleration fields. The acceleration was up to 10g and the heat load ranged from 100 W to 600 W. It was found that there was a transient periodic flow reversal in the loop for some cases, which was likely resulted from vapor bubble forming in the primary wick. Yerkes et al. [25] studied the transient operating performance of a titanium-water LHP subjected to a steady-periodic acceleration filed in the form of a sine wave by experiments. The radial acceleration value and frequency of the sine wave ranged from 0.5g to 10g and 0.01Hz to 0.1 Hz. It was found that the natural oscillation of the fluid in the condenser appeared. The steady-periodic acceleration resulted in a steady-periodic operating behavior. In our previous work [26, 27], temperature oscillations were revealed on a DCCLHP under both constant acceleration and periodic acceleration conditions. For the case of constant acceleration [26], periodic temperature oscillations are normally appeared on almost all the loop at 250 W and 300 W when the acceleration force pointed to the CC1 from the CC2 along the axis of the evaporator. While during the periodic acceleration period [27], the loop temperature showed a periodic oscillation with the periodic change of the acceleration. Furthermore, the effect of different heat loads, loading modes periodic acceleration patterns and acceleration directions on the operating behavior of the DCCLHP were analyzed in periodic acceleration fields.

It appears from the previous investigations that there are only limited reports on the temperature oscillation of DCCLHP. To the best of the authors' knowledge, however, both theoretical and experimental investigations on the temperature oscillation of DCCLHP under the acceleration fields have been far from complete and there is still much room to be enhanced in this area. There is also a lack of available experimental data concerning the temperature oscillation of DCCLHP under acceleration fields. As such, the objective of the current work is to address the temperature oscillation of DCCLHP subjected to various heat loads and acceleration magnitudes as well as different acceleration directions under constant acceleration conditions. Furthermore, the transient characteristics of the DCCLHP subjected to constant acceleration forces will also be discussed.

## 2. EXPERIMENTAL DESCRIPTIONS

### 2.1. Experimental apparatus

A LHP performance test apparatus was constructed and experimental studies were carried out to determine the operating performance of an ammonia-stainless steel DCCLHP under constant acceleration conditions at the Reliability and Environmental Engineering Laboratory at Beihang University, Beijing, China. In the current work, the actual details of the test apparatus were consistent with the previous study of Xie et al. [26, 28] and will only be described briefly here for the purpose of completeness.

The experimental system mainly consisted of four subsystems: the acceleration simulating and control subsystem, data acquisition and control subsystem, water cooling circulation subsystem as well as test section. Fig. 1 depicts the schematic diagram of the experimental apparatus and configuration of the test section. The acceleration force was generated by the clockwise rotation of the rotary arm of the centrifuge in the acceleration simulating and control subsystem. There were two rotary arms on opposite sides of the centrifuge axis and the maximum turning diameter was about 4.5 m. The maximum radial acceleration magnitude up to 11g could be achieved under rotation. The rotational speed with an accuracy of  $\pm 5\%$  can be adjusted by the acceleration controller. During the experiment, the maximum continuous operating duration was limited to one hour and the maximum acceleration magnitude was limited to 9g due to safety concerns. The stationary and rotational components of the fluid tubes, electrical wires and signal wires were linked up well through the liquid collecting rings and the electric slip rings.

In the water cooling circulation subsystem, the cooling water with a temperature of 19 °C was driven by a gear pump flowed out of the thermostatic water tank and then passed through a filter, a mass flow meter with an accuracy of  $\pm 0.5\%$  (DMF-1-2), an aluminum cold plate (type 6061) and plate heat exchanger. After that, it flowed back to the tank. In the data acquisition and control subsystem, a resistance temperature detectors (RTDs) Pt100 were used to monitor the temperature along the loop. All the collected temperature and mass flow rate were recorded, displayed and stored by the Agilent 34970A. A flexible polyimide film electric resistance heater was used to apply the heat load with a range of 0-300 W on the evaporator of the DCCLHP. The DC power supply (DH1716A-13) was used to provide the power for the heater with output voltage ranges of 0 to 250 V and output current changes from 0 to 5 A, respectively.

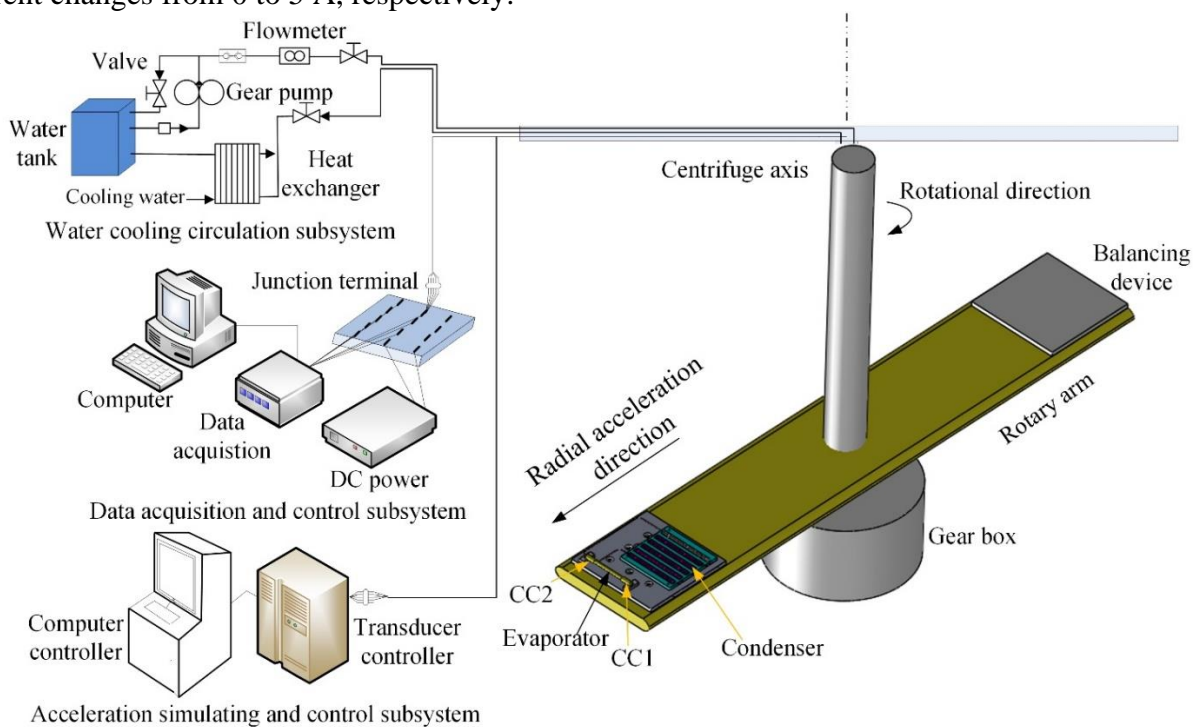


**Fig. 1.** Schematic diagram of experimental apparatus and configuration of test section.

## 2.2. Test section

In the current work, the test section was an ammonia-stainless steel DCCLHP with a bayonet that was designed and manufactured by the Chinese Academy of Space Technology [26]. It mainly consisted of an evaporator, two CCs, condenser, vapor line and liquid line, as shown in Fig. 2. The overall dimension of the DCCLHP was 565 mm in length, 469 mm in width and 25 mm in height. A nickel wick with the maximum pore radius of  $1.5\ \mu\text{m}$  was sealed inside the evaporator envelope. The wick was fabricated by powder metallurgy sintering using T255 nickel powder as raw material. The particle size of nickel powder is about  $3\sim 4.5\ \mu\text{m}$ . After performed by pure physical pressure, the preformed capillary wick was put into a graphite furnace for sintering with approximate  $400\ ^\circ\text{C}$ . Argon gas was introduced to protect the wick from oxidation during sintering. The bayonet extending to the midpoint of evaporator core was used to drive the vapor bubbles away from the evaporator core at any orientation. All the transport lines including the condenser lines were stainless steel smooth-walled tubes and the outer diameter was 3.0 mm. The major design parameters of the test section are listed in Table 1.

For the purpose of reference, CC2 and CC1 respectively refer to the compensation chamber with the bayonet passing through and without. The DCCLHP was arranged inside a stainless steel enclosure along with the film electric resistance heater and the cold plate, as demonstrated in Fig. 3. The copper heat expansion fins welded with the condenser line were closely attached on the surface of the cold plate. The thermal grease was used to reduce the contact resistance between the cold plate and heat expansion fins. In order to prevent the heat loss from the surroundings as much as possible, multilayer insulation materials were used to wrap all the components of the DCCLHP with glass wool crammed into the enclosure.

In the current study, two loading modes were used to apply both the acceleration force and heat load on the DCCLHP. The first loading mode was defined as the heat load was applied firstly, after which the loop reached a steady state then the acceleration force applied. The second loading mode was defined for both the heat load and acceleration force were applied simultaneously. In addition, there are two different arrangements of temperature measuring points on the condenser line for both loading modes. Fig. 4 schematically presented the detailed allocations of the RTDs. RTD1 and RTD2 were placed on the CC1 and CC2 respectively. RTD3 was used to monitor the evaporator temperature. RTD4 was placed at the outlet of the vapor line. RTD5 to RTD9 were attached on the outer wall of the straight line for the first loading mode, while RTD5' and RTD6' on the outer wall of the bend for the second loading mode. RTD10, RTD11 and RTD12 were used to monitor the temperature of the inlet, middle and outlet of the liquid line.

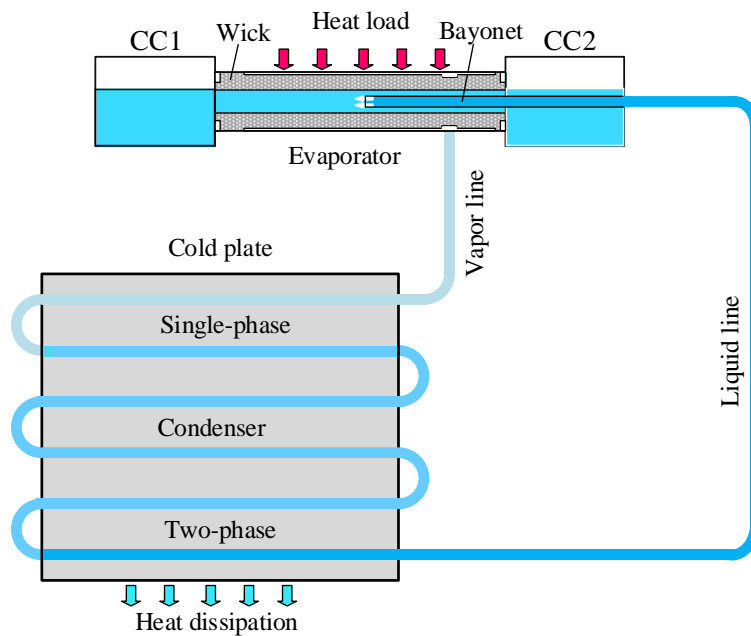


**Fig. 2.** The overall schematic of the DCCLHP.

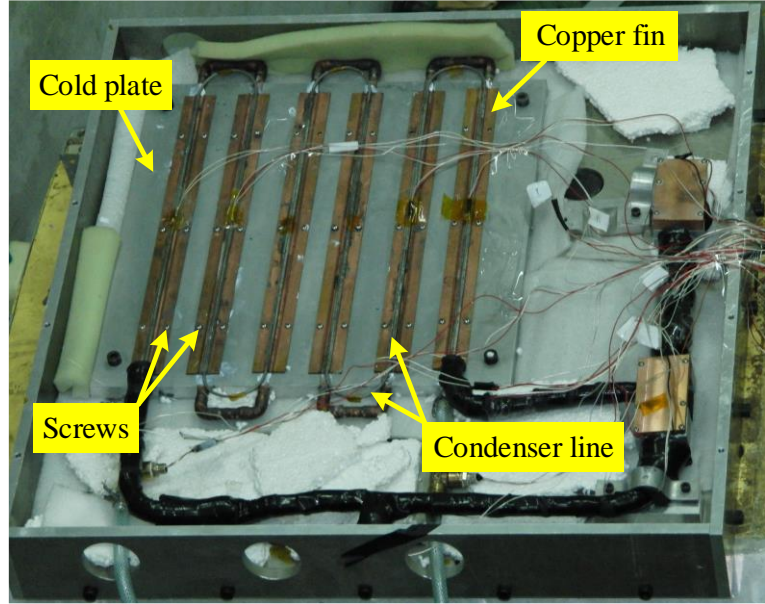


**Fig. 3.** The DCCLHP in the enclosure.

**Table 1.** Design parameters of the test section.

	Component	Parameter	Material
Evaporator	O.d./i.d.× Length	20 mm/18 mm × 209 mm	Stainless steel
Wick	Pore radius	<1.5 μm	
	Porosity	55%	
	Permeability	$>5 \times 10^{-14} \text{ m}^2$	Nickel
	O.d./i.d.× Length	18 mm/6 mm × 190 mm	
Vapor line	O.d./i.d.× Length	3 mm/2.6 mm × 225 mm	Stainless steel
Liquid line	O.d./i.d.× Length	3 mm/2.6 mm × 650 mm	Stainless steel
Condenser line	O.d./i.d.× Length	3 mm/2.6 mm × 2200 mm	Stainless steel
CC	O.d./i.d.× Length	27 mm/25 mm × 64 mm	Stainless steel
	Number	2	
Working fluid		Ammonia	

### 2.3. Test procedure

Prior to the real test, all the instruments and RTDs were calibrated. For a given acceleration direction, the test section was mounted horizontally on the rotary arm. In the current study, there were four different acceleration directions, defined as configuration A, B, C and D, as demonstrated in Fig. 4. For configuration A and C, the radial acceleration direction was consistent with the evaporator axial line. As a consequence, the acceleration force vector pointed to CC2 from CC1 under configuration A, while pointed to CC1 from CC2 under configuration C. For configuration B and D, the acceleration direction was perpendicular to the evaporator axial line. The evaporator was placed at the inner edge of the rotary arm under configuration B while at the outer edge under configuration D. Different configurations could be converted by rotating the test section through 90 degrees using the rotary arm as a reference.

For all the tests, six different heat loads ( $Q_e=25 \text{ W}, 80 \text{ W}, 150 \text{ W}, 200 \text{ W}, 250 \text{ W}, 300 \text{ W}$ ) and five radial acceleration magnitudes ( $a=1g, 3g, 5g, 7g, 9g$ ) were taken into account. As is always the case, the gravity should be considered in all tests. For the tests under the first loading mode, the inlet temperature of the cold plate was maintained at temperature of 19.8 °C~20.8 °C, while for the tests under the second loading mode, the inlet temperature of the cold plate was maintained at temperature

of 20.1 °C~22.2 °C. The ambient temperature was maintained at temperature of 24.1 °C~27.5 °C by air conditioning.

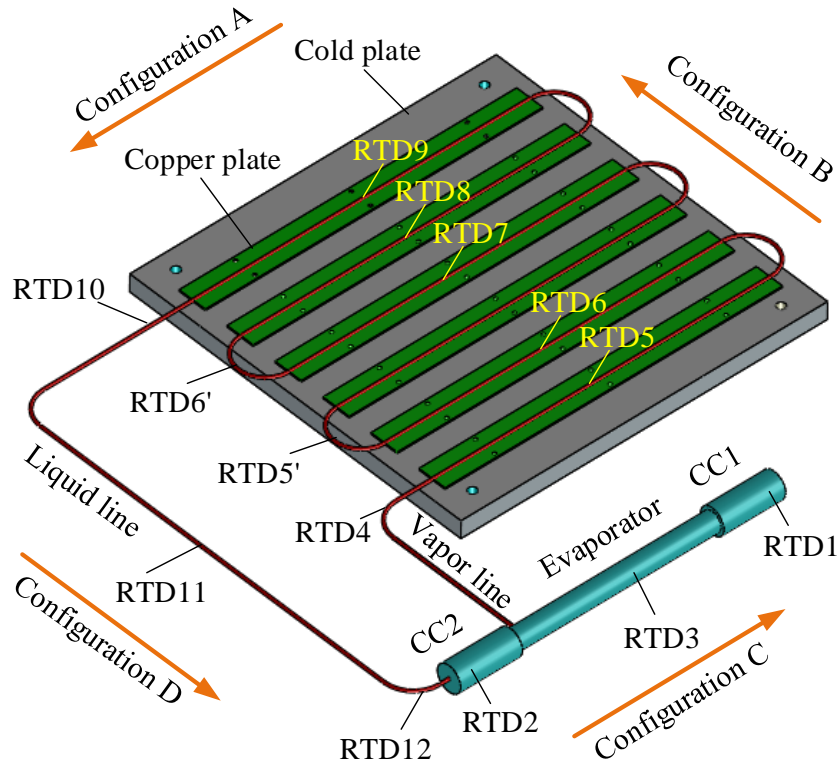


**Fig. 4.** Locations of RTDs on the DCCLHP and acceleration direction sketch.

### 3. EXPERIMENTAL RESULTS AND DISCUSSION

#### 3.1. Impact of heat loads

Fig. 5 shows the temperature profiles of the DCCLHP at 5g under configuration B with first loading mode at four different heat loads i.e. 150W, 200 W, 250 W and 300 W. It should be noted that the temperature of the liquid line oscillates only at 250 W and 300 W under terrestrial gravity. Feng et al. [15] also found similar temperature oscillation at 270 W. The evaporator temperature under terrestrial gravity is 45.8 °C, 40.1 °C, 39.9 °C and 43.8 °C at 150 W, 200 W, 250 W and 300 W respectively, while it is 42 °C, 40.4 °C, 40.2 °C and 42.7 °C at 5g.

When the acceleration is applied, the temperature of the liquid line changes insignificantly with heat load of 150 W and 200 W, as depicted in Fig. 5(a) and (b). While the temperature of the liquid line drops rapidly with 5~10 °C during a short period, as presented in Fig. 5(c) and (d). Then it rises gradually with slight oscillation. This could be the reason that the oscillatory state for the cases of 250 W and 300 W is broken up due to acceleration force. The vapor-liquid interface moves back and forth at the outlet of the condenser according to the RTD8~RTD10 temperature under terrestrial gravity. The acceleration causes the vapor and liquid working fluid to be redistributed in the loop. The interface moves back into the condenser and the liquid is supercooled. In the meantime, the external pressure head of the loop increases as a result of the acceleration force. The increased temperature in the evaporator will enlarge the capillary force in order to circulate the fluid. As a result, the subcooling liquid enters into the liquid line and the temperature drops sharply. The subcooling of the liquid can lead to the temperature oscillation in the loop to be restrained.

In addition, the evaporator temperature increases and then drops for the cases of 200 W, 250 W and 300 W when the acceleration is applied. The temperature of the CC2 drops and then increases to 36.4 °C and 34.2 °C at 150 W and 200 W, respectively. While it oscillates to 33.8 °C and 35.6 °C at 250 W and 300 W, respectively. At the end of test, the evaporator and CCs do not show temperature oscillation.

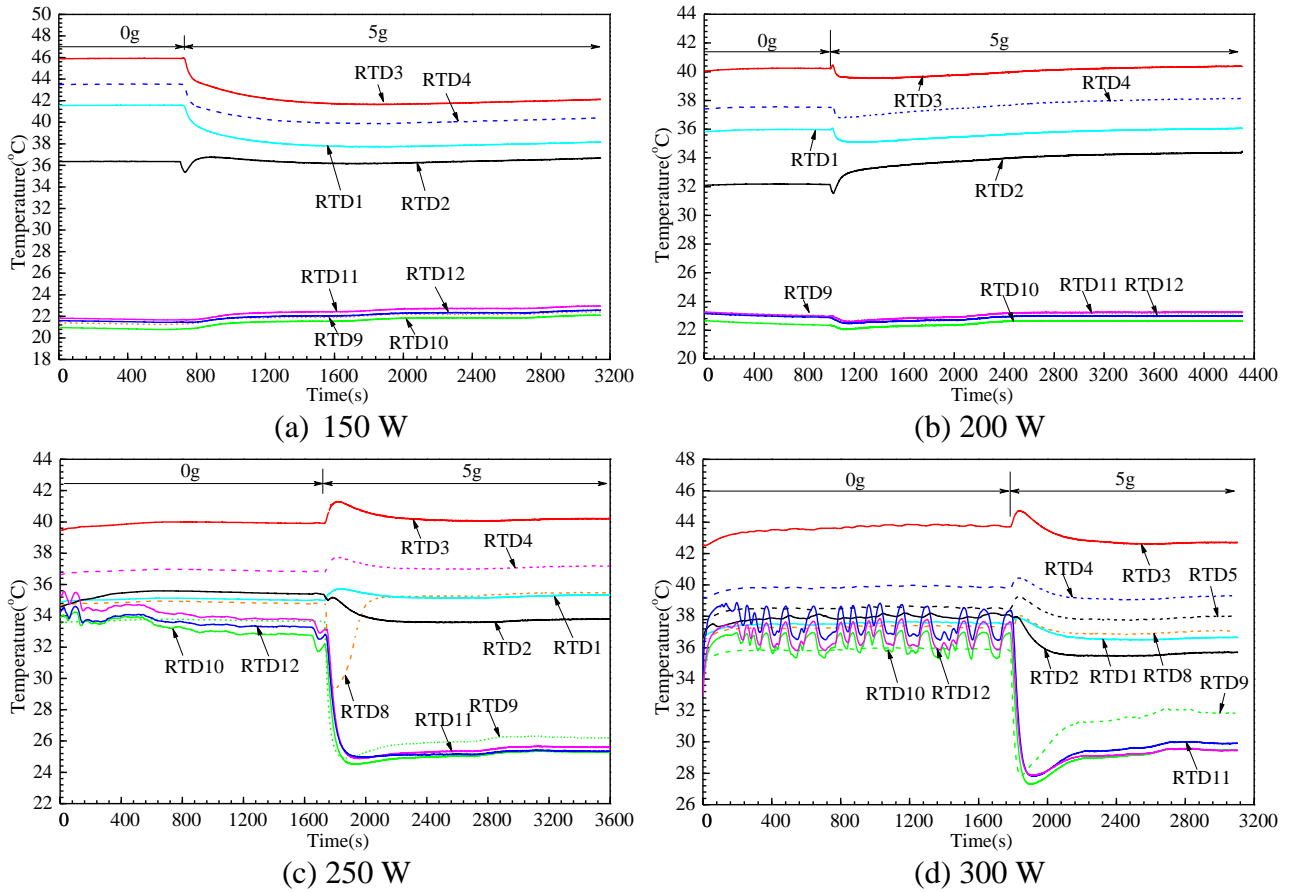


**Fig. 5.** Temperature profiles of the DCCLHP at 150 W, 200 W, 250 W and 300 W under configuration B, 5g and first loading mode.

Fig. 6 presents the temperature profiles of the loop at 5g under configuration C with the second loading mode under four different heat loads i.e. 150 W, 200 W, 250 W and 300 W. As shown in Fig. 6, it can be seen clearly that the temperature oscillation occurs with the increase of the heat load. During the initial period of the test, the temperature of the liquid line decreases initially and then increases for each heat load.

In Fig. 6(a), as the acceleration is applied, the vapor-liquid distribution in the loop changes due to the acceleration force. The liquid with low temperature in the condenser will be pushed into the liquid line by the acceleration force. Thus, the temperature of the liquid line drops, followed by the vapor-liquid interface moves towards the outlet of the condenser since the vapor generates in the evaporator. The temperature of the liquid entering into the liquid line increases. Afterwards, the interface moves back and the liquid temperature at the inlet of the liquid line drops again. During the period of 205 s to 340 s, only the outlet temperature of the liquid line oscillates. This phenomenon could be introduced by the warm vapor reverse flow from the evaporator core. At the end of test, the temperature of the liquid line is kept at about 21.6 °C. It can also be seen that the temperature of the evaporator and CCs does not oscillate during the test.

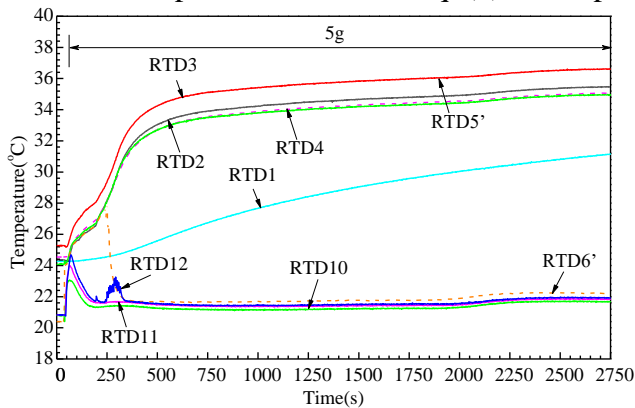
For the case of 200 W, as shown in Fig. 6(b), after the heat load and acceleration force are applied, the RTD3, RTD4 and RTD5' temperatures rise immediately. It indicates that the vapor generates and enters into the condenser. Concurrently, the cooled liquid in the condenser moves into the liquid line due to inertia, this could lead to the RTD10, RTD11 and RTD12 temperature drops. Afterwards, the condensation length in the condenser increases gradually and the subcooling of the liquid decreases. As a sequence, the RTD10, RTD11 and RTD12 temperature increase rapidly. Since the interface moves back and forth in the condenser, the RTD10, RTD11 and RTD12 temperature oscillates persistently. Moreover, the subcooling of the liquid returning to the CCs changes persistently. Thus, the temperature of the evaporator and CC2 also oscillates upward. The oscillatory amplitude of the loop gradually increases with time and the maximum temperature of 4.5 °C is achieved. The CC1 is

filled with the liquid by the acceleration force and the CC1 temperature does not oscillate. However, the temperature oscillation of the loop disappears at about 550 s. This could be explained by the fact that the CC2 reaches an energy balance as the minimum condensation length in the condenser occurs. The evaporator temperature gradually increases to 33.6 °C.

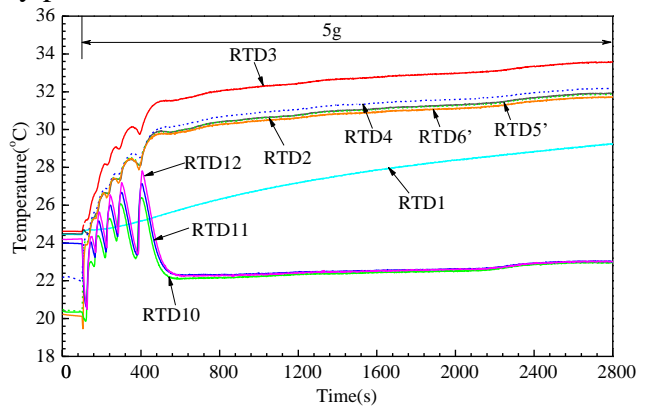
When the heat load is 250 W, as shown in Fig. 6(c), the temperature of the entire loop except for the CC1 shows obviously periodic oscillation after the DCCLHP starts up. During the initial period of the oscillation, the temperature profile at 250 W is similar to that for the case of 200 W. But after about 380 s, the oscillatory amplitude increases gradually and the frequency decreases. It is clearly seen that the amplitude on the liquid line is much larger than that on the other loop components. Furthermore, the amplitude of the RTD10 is smaller than that of the RTD11. The amplitude of the RTD10 is smaller than that of the RTD12. The maximum amplitude of the RTD10, RTD11 and RTD12 temperature is 4.5 °C, 4.8 °C and 5.8 °C, respectively. The temperature oscillation of the loop has almost the same period and the oscillation pattern is an asymmetric pattern. For example, it takes about 94 s for the RTD12 temperature to decrease from the peak to the valley, while it takes 50 s to increase from the valley to the peak. Eventually, the DCCLHP reaches a periodically oscillatory state. The peak and valley temperature of the evaporator are 35.4 °C and 34.4 °C, respectively.

In Fig. 6(d), when the heat load increases to 300 W, a periodic oscillation of the entire loop temperature can be observed, which is similar to the case of 250 W. After the DCCLHP starts up, the amplitude of each loop component increases gradually. The loop reaches a periodically oscillatory state. The valley and peak value of the inlet temperature of the liquid line are about 32.9 °C and 34.2 °C, respectively. The oscillatory pattern is asymmetric with the total period of 36 s. It can also be seen that the valley and peak of the evaporator temperature are about 38.1 °C and 38.4 °C, respectively. The oscillatory period of the evaporator temperature is the same as that of the temperature of the liquid line. However, it shows a 180 degrees out of phase between the evaporator and liquid line. Compared with the case of 250 W, as plotted in Fig. 5(c), the amplitude and period at 300 W are smaller than those at 250 W.

It should be noted that it is important to explore the physical mechanism of the above periodic temperature oscillation of the loop. Since DCCLHP is a two-phase flow and heat transfer device, the coupling effects normally occurs among its various components such as evaporator, CCs and condenser. As the inlet temperature of the liquid line starts to increase from the valley, the condensation length of the condenser starts to increase. The vapor-liquid interface would move forward gradually to the inlet of the liquid line. The liquid substituted by the advancing vapor in the condenser is pushed into the liquid line. Correspondingly, the pressure head resulted from the acceleration force would decrease under configuration C. In order to satisfy the pressure balance of the whole loop, as shown in the Eq. (1), the capillary pressure difference of the wick reduces.



(a) 150 W



(b) 200 W

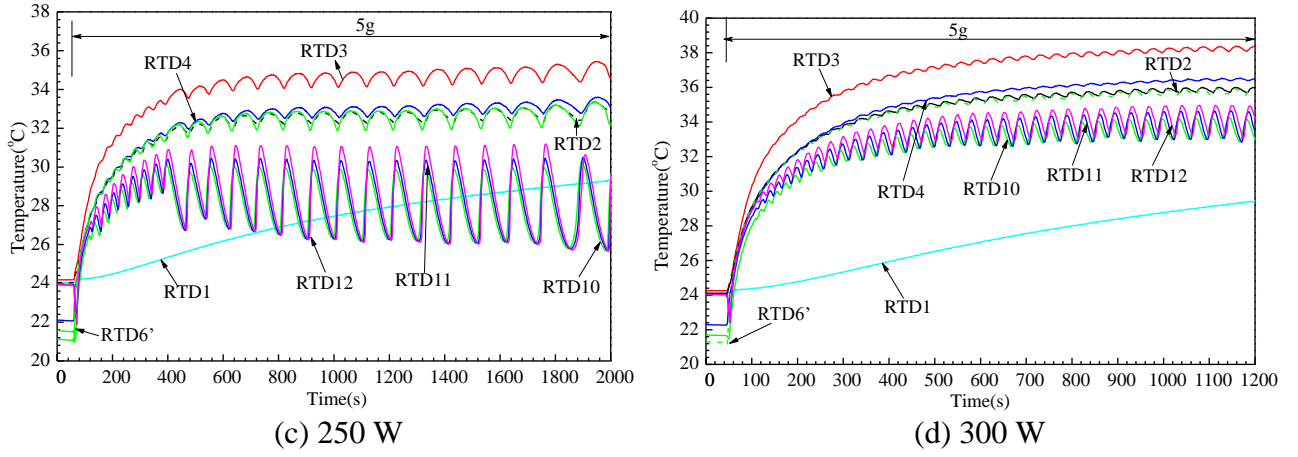


**Fig. 6.** Temperature profiles of the DCCLHP at 150 W, 200 W, 250 W and 300 W under configuration C, 5g and second loading mode.

$$\Delta P_{\text{cap}} = \Delta P_{\text{vg}} + \Delta P_{\text{vl}} + \Delta P_{\text{cond}} + \Delta P_{\text{ll}} + \Delta P_{\text{bay}} + \Delta P_{\text{wick}} + \Delta P_{\text{a}} \quad (1)$$

where  $\Delta P_{\text{cap}}$  is the capillary force of the wick.  $\Delta P_{\text{vg}}$ ,  $\Delta P_{\text{vl}}$ ,  $\Delta P_{\text{cond}}$ ,  $\Delta P_{\text{ll}}$ ,  $\Delta P_{\text{bay}}$  and  $\Delta P_{\text{wick}}$  is the pressure drop in the vapor grooves, vapor line, condenser, liquid line, bayonet and wick, respectively.  $\Delta P_{\text{a}}$  is the additional pressure head in the external loop by the acceleration force, which depends on the position of the vapor-liquid interface in the condenser.

Therefore, according to the Clausius-Clapeyron relationship shown in Eq. (2):

$$P_{\text{evap}} - P_{\text{CC}} = \frac{h_{\text{fg}}}{T v_{\text{fg}}} (T_{\text{evap}} - T_{\text{CC}}) \quad (2)$$

where  $P_{\text{evap}}$  and  $T_{\text{evap}}$  is the pressure and temperature at the vapor side of the meniscus.  $P_{\text{CC}}$  and  $T_{\text{CC}}$  is the pressure and temperature in the CC.  $h_{\text{fg}}$  is the heat of vaporization of the working fluid,  $v_{\text{fg}}$  is the difference between the vapor and liquid specific volumes. The temperature difference between the liquid-vapor interfaces in the evaporator and in the compensation chamber will also decrease. This in turn reduce the heat leak from the evaporator to the CC2. According to the energy balance of the CC, the temperature of CC2 drops. Thus the evaporator temperature also drops.

The loop pressure balance is rebuilt up to the temperature of the CC2 gets to its valley value. Simultaneously, the temperature of the evaporator also decreases to its valley value. According to the temperature of the condenser and the liquid line in Fig. 6, there is an approximate 180° phase difference between the evaporator and liquid line. Thus the vapor-liquid interface rushes out of the condenser and moves forward to somewhere in the liquid line. At this moment, the subcooling of the liquid reduced to the minimum value. Along with the interface gradually reaches the maximum distance far from the exit of the condenser, the liquid in the external loop floods into the evaporator core and CCs. Simultaneously, the additional pressure drop by the acceleration force gradually gets to the minimum value. Correspondingly, the pressure in the CC2 will increase to the maximum value. The pressure difference between the evaporator and CC2 will decrease. Consequently, the interface will move back toward the condenser due to lack of driving force.

Once the interface moves back towards the condenser, the additional pressure drop resulted from the acceleration force increases. The capillary pressure difference increases to balance the additional pressure drop. According to Eq. (2), the temperature difference between the liquid-vapor interfaces in the evaporator and in the CC increases as well. This in turn enlarges the heat leak from the evaporator to the CC2. As a consequence, the temperature of the CC2 and evaporator increases. In the meantime, the subcooling of the liquid increases which leads to the temperature of the liquid line drop. When the interface moves back to somewhere between RTD6' and RTD10 point in the condenser, the condensation length reaches the minimum value and the subcooling of the returning liquid reaches the maximum value. It causes the CC2 temperature to stop increasing and begin to drop. Correspondingly, the next cycle of the loop starts.

It should be stressed here, however, that the fundamental mechanism of the temperature oscillation of the DCCLHP is not clear due to its inherent complexity and instability of two phase flow and heat transfer. Especially under acceleration conditions, the acceleration effect makes the two phase flow and heat transfer more complicated. It is imperative, therefore, to explore the physical mechanism and any new phenomena pertinent.

According to the above results, it can be found that the loop temperature at 250 W and 300 W oscillates periodically under both terrestrial and acceleration conditions. While for most of the cases, the temperature of the liquid line always shows obvious oscillation since the vapor-liquid interface moves back and forth at the outlet of the condenser.

### 3.2. Impact of loading modes

As shown in Figs. 5 and 6, the operational behavior of the DCCLHP shows obvious difference under both loading modes. Thus, the impact of the loading modes on the temperature oscillation is discussed as follows.

Fig. 7 depicts the temperature evolutions of the loop for the cases of 250 W and 300 W at 5g under configuration A with both loading modes. For the first loading mode, the loop temperature decreases when the acceleration is applied. The evaporator temperature finally keeps a constant. While for the second loading mode, only the temperature of the liquid line decreases as the acceleration is applied. The evaporator temperature gradually increases.

It can be found from Fig. 7(a) and (b) that the temperature of the liquid line oscillates at the second loading mode, whereas it changes very little at the first loading mode. In Fig. 7(a), the evaporator temperature gradually decreases to 40.2 °C. Compared to the CC1 temperature, the CC2 temperature drops sharply and is kept at 27.8 °C finally. In Fig. 7(b), the evaporator temperature increases gradually and finally reaches to about 40.6 °C. The temperature of the liquid line drops initially and then increases to about 30 °C~30.6 °C. Afterwards, it shows a trend of oscillating downward.

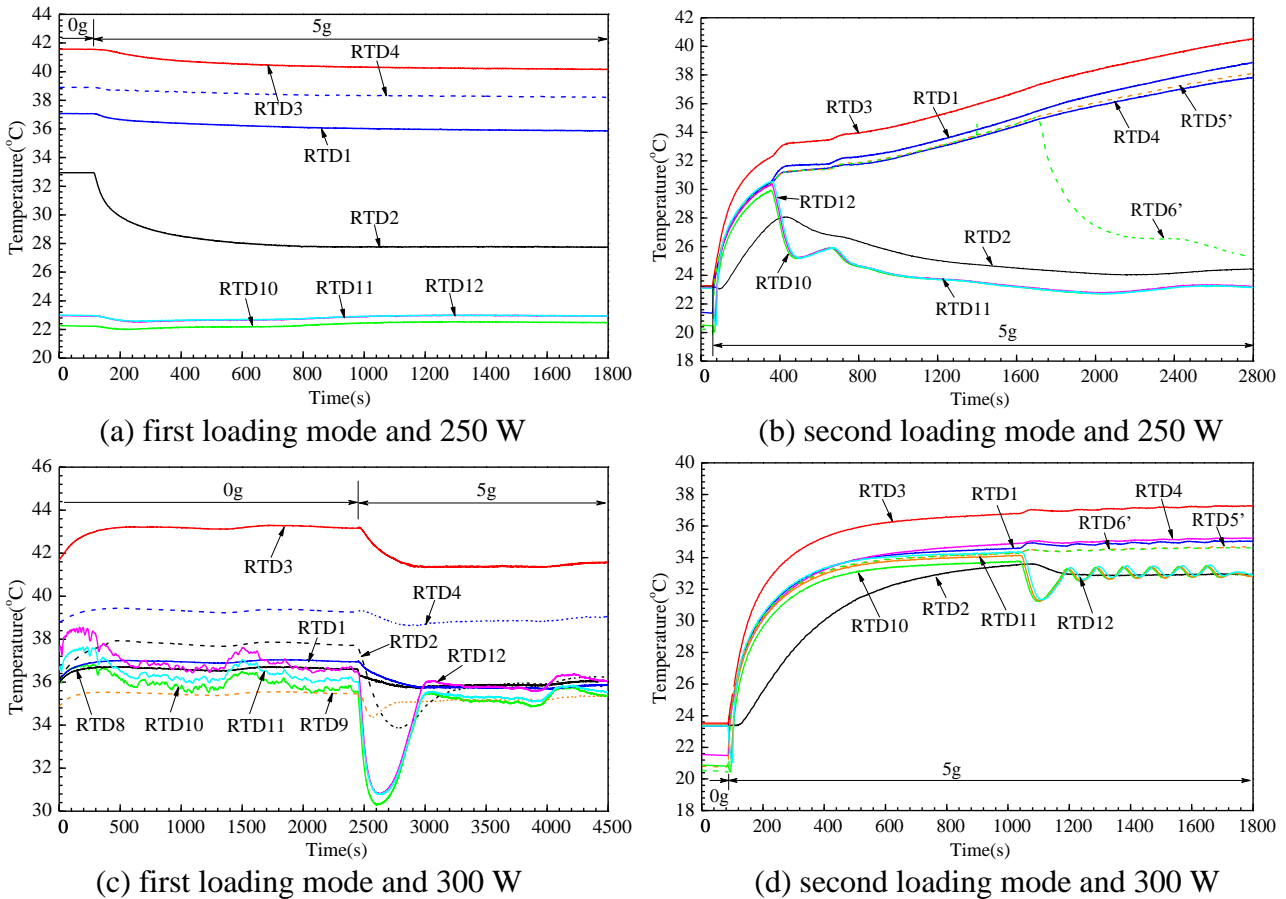


**Fig. 7.** Temperature evolutions of the DCCLHP with 250 W and 300 W at 5g under configuration A for both loading modes.

At 300 W, the liquid line shows an obvious oscillatory temperature under terrestrial gravity, as shown in Fig. 7(c). Both CCs and condenser do not present temperature oscillation. The vapor-liquid interface locates near the exit of the condenser in terms of the RTD8, RTD9 and RTD10 temperature. When the acceleration is applied, the temperature of the liquid line drops sharply close to 30.4 °C followed by a rapid increase to about 36.0 °C. The CC2 temperature also drops and then increases. The reason can be addressed as follows. The vapor and liquid working fluid in the loop are firstly redistributed by the acceleration force. In the condenser, the liquid condensed from part of vapor is pushed towards the side of the liquid line. The interface returns back into the condenser in the meantime. Thus the liquid will be subcooled as flowing out of the condenser. Furthermore, the acceleration effect could drive liquid to form a thinner liquid layer in the two phase region in the condenser, which could lead to the increase of the heat transfer coefficient. Therefore, the temperature of the RTD10, RTD11 and RTD12 shows a high jump as the subcooled liquid reaches the corresponding position. In the evaporator and CCs, the CC2 will accumulate more liquid and the CC1 will be filled with more vapor. This vapor-liquid distribution further leads to the decrease of the heat leak from evaporator to CCs. Consequently, the RTD1 and RTD2 temperature drops. Combining the cooling of the returning liquid, the temperature drop of the RTD2 is larger than that of RTD1. the temperature drop of the RTD2 is larger than that of RTD1. Due to the subcooled liquid locates in the condenser, an additional pressure head is generated by the acceleration force. The interface will be pushed towards the exit of the condenser by the large capillary force and additional pressure head. As a result, the subcooling of the liquid decreases. The RTD10, RTD11 and RTD12 temperature increases in turn. During the acceleration, the temperature oscillation of the liquid line persists. The evaporator temperature decreases from 43.2 °C to 41.3 °C.

In Fig. 7(d), the evaporator temperature increases immediately when the heat load is applied. In the meantime, the vapor-liquid distribution in the loop is changed due to the effect of the acceleration. The RTD10 temperature increases slightly and then decreases along with the temperature of RTD11 and RTD12. At about 1040 s, the temperature of the liquid line starts to oscillate, in the meantime, the temperature of the evaporator, vapor line and CC1 oscillates slightly. After the fluctuation with about 500 s, the amplitude further decreases at about 1700 s.

Fig. 8 shows the temperature evolutions of the DCCLHP with heat load of 250 W and 300 W at 5g under configuration C for the first loading mode. As shown in Fig. 8, the temperature of the loop changes significantly when the acceleration is applied. During the initial period, the temperature of the liquid line shows large jump with large amplitude. The evaporator temperature under acceleration condition is smaller than that under terrestrial gravity. During the late stage of the test, the temperature of the liquid line shows little oscillation, whereas the evaporator temperature does not show any oscillation. At the end of test, the evaporator temperature at 250 W and 300 W is 39.7 °C and 43.6 °C, respectively.

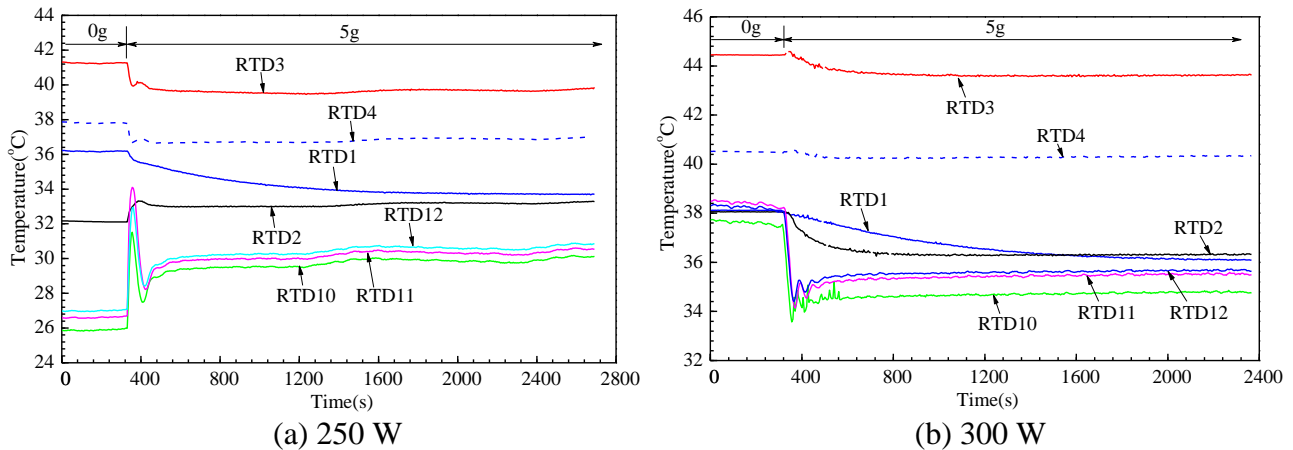


**Fig. 8.** Temperature evolutions of the DCCLHP with 250 W and 300 W at 5g under configuration C for first loading mode.

Compared Fig. 8(a) with Fig. 6(c), as well as Figs. 8(b) with Fig. 6(d), a significant periodic oscillation of the entire loop occurs for the second loading mode under configuration C. For the first loading mode, only the temperature of the liquid line presents an obvious jump when the acceleration force is applied. After approximate 600 s, as shown in Fig. 8, the temperature of the liquid line oscillates slightly.

In summary, it is believed that the temperature jump appears for the case of the first loading mode when the acceleration is applied. There exists a large temperature jump in the liquid line but small in the evaporator. However, for the second loading mode, the temperature of the liquid line always oscillates when the acceleration is applied. At some cases, the temperature of the evaporator and CCs can also present a periodic temperature oscillation together with the liquid line. For both loading modes, the vapor-liquid redistribution and the change of two phase flow and heat transfer by the acceleration effect are the primary reason leading to the temperature jump and temperature oscillation.

### 3.3. Impact of acceleration direction

For the first loading mode, the experiments have been performed under four different configurations, whereas for the second loading mode, only configurations A, C and D are investigated in the current work. Table 2 lists the results of the temperature oscillation of the loop at 5g and 7g under four different configurations for both loading modes.

For the first loading mode at 7g, the DCCLHP under configuration A and B does not oscillate at 150 W, 200 W and 250 W. While the DCCLHP under configuration C does not oscillate at 200 W. The loop does not oscillate at 150 W and 200 W under configuration D. It should be noted that the temperature oscillation always occurs on the liquid line during the initial period of the acceleration. For configuration B, the temperature oscillation can be repressed by the effect of the acceleration according to Figs. 5(c) and (d).

**Table 2.** Temperature oscillation of the loop under different configurations

Case		Configuration A	Configuration B	Configuration C	Configuration D
First loading mode, 7g	150 W	N.	N.	Y.	N.
	200 W	N.	N.	N.	N.
	250 W	N.	N.	Y.	Y.
	300 W	Y	Y	Y	Y
Second loading mode, 5g	25 W	Y	-	Y	Y, All loop
	80 W	Y	-	Y	N
	150 W	Y	N	Y	Y, All loop
	200 W	Y	N	Y, All loop	Y
	250 W	Y	N	Y, All loop	Y
	300 W	Y	N	Y, All loop	Y

Note: N refers to no oscillation. Y mainly refers to temperature oscillation of the liquid line. All loop refers to periodic temperature oscillation of the entire loop.

As for the second loading mode at 5g, the temperature oscillation of the DCCLHP under configuration A, C and D occurs at all heat loads except for 80 W. However, the temperature oscillation does not occur under configuration B. Under configuration A, the temperature oscillation occurs mainly on the liquid line. Periodic temperature oscillation of the entire loop appears significantly under configuration C at 200 W, 250 W and 300 W. It also occurs at 25 W and 150 W under configuration D, whereas it does not oscillate at 80 W under configuration D.

### 3.4. Impact of acceleration magnitude

Fig. 9 presents the temperature profiles of the loop with 300 W under configuration C for the case of second loading mode at four different accelerations i.e. 3g, 5g, 7g, and 9g. It can be clearly seen

from Fig. 9 that periodic temperature oscillation of the entire loop with high frequency and low amplitude occurs at four different acceleration magnitudes. For a given acceleration magnitude, the amplitude of the liquid line is significantly larger than that of the evaporator. Ku [23] also presented similar results for a single CC LHP. The oscillatory period of the liquid line is almost the same as that of the evaporator. But the phase difference of the evaporator and the liquid line is nearly 180 degrees. This phenomenon is the same as that reported by Chen [11]. Moreover, the wave pattern of each component of the loop is asymmetric in a certain period of time. Due to the CC1 is filled with the subcooling liquid of the working fluid, the temperature of the CC1 does not oscillate. The amplitude and period of the liquid line and evaporator show a trend of decrease with the increase of the acceleration magnitude. Finally, the DCCLHP reaches a periodically oscillatory state.

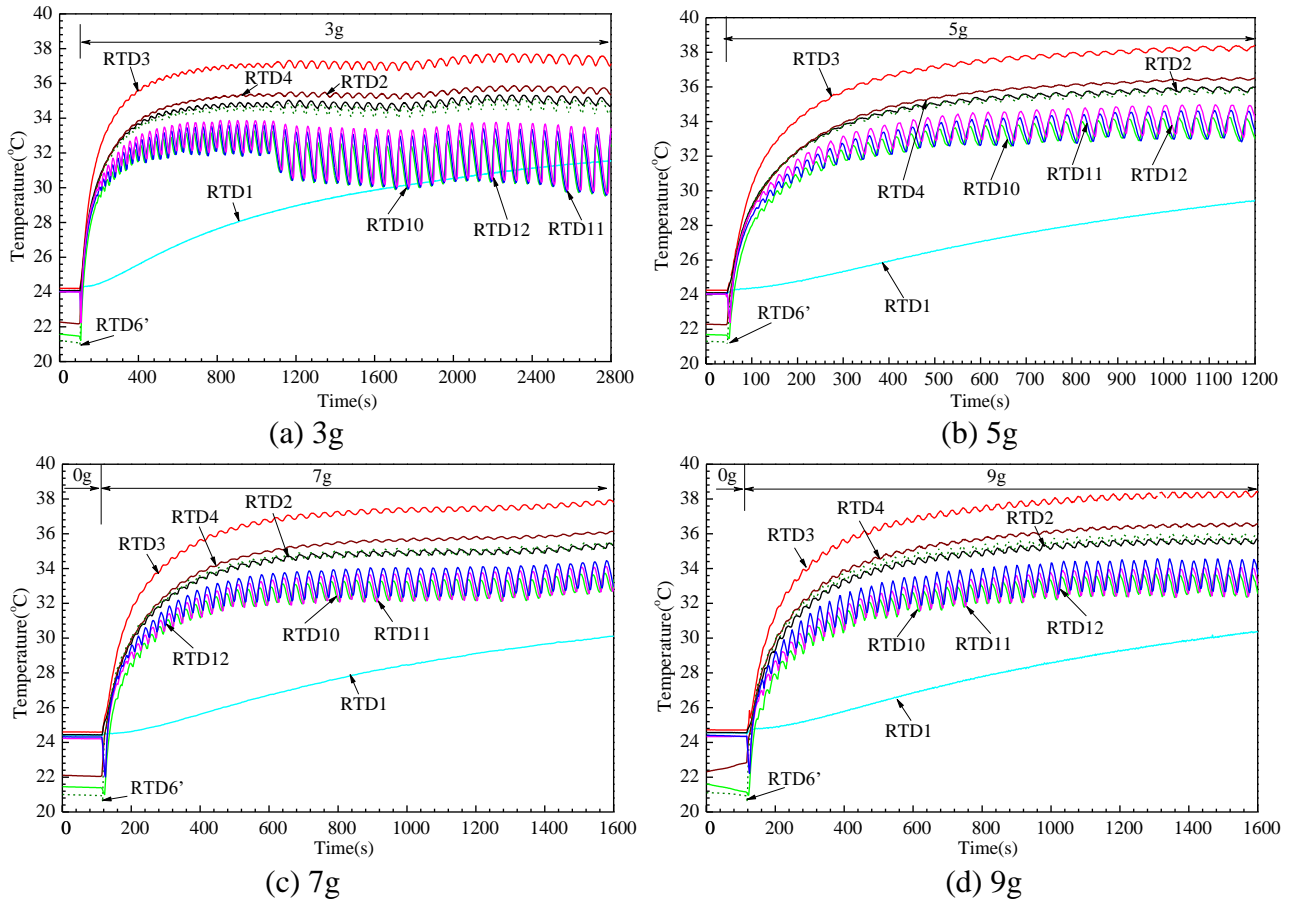


**Fig. 9.** Temperature evolutions of the loop with 300 W at 3g, 5g, 7g, 9g under configuration C and second loading mode

In Fig. 9(a), it is at approximately 1100 s that the amplitude and period of the loop suddenly increases. Among the components of the DCCLHP, the amplitude of the liquid line is the largest. The amplitude of the evaporator and CC2 is almost identical. At the end of test, the evaporator temperature varies from 37.0 °C to 37.6 °C. The amplitude and period of the evaporator temperature are about 0.6 °C and 66 s, respectively. The amplitude of the RTD10 temperature is approximate 1.8 °C and the period is 66 s. The amplitude of the RTD12 temperature is approximate 3.6 °C and the period is also 66 s. When the acceleration increase to 5g, as shown in Fig. 9(b), the DCCLHP starts to oscillate after startup and finally gets to an oscillatory state. For the evaporator, the amplitude and period of the temperature oscillation are approximate 0.3 °C and 36 s, respectively. The amplitude of the CC2 is almost the same as that of the evaporator. For the liquid line, the amplitude of its inlet temperature and outlet temperature is about 1.4 °C and 1.5 °C respectively. The wave pattern of the RTD10, RTD11 and RTD12 is asymmetric with the total period of 36 s.

In Fig. 9(c), the temperature oscillation of the DCCLHP is weakened in comparison to the case of 3g. The amplitude of the evaporator is very small with around 0.2 °C and the period is approximate

34 s. The amplitude of the RTD10 and RTD12 is 1.2 °C and 1.6 °C, respectively. When the acceleration magnitude increases to 9g, as shown in Fig. 9(d), the oscillation is similar to that at 7g. The evaporator temperature varies from around 38.1 °C to 38.4 °C with the total period of 36 s. The temperature of the RTD10 and RTD12 changes from about 32.4 °C to 33.7 °C and 32.6 °C to 34.5 °C, respectively.

According to the above results, the oscillatory amplitude and period of the loop temperature show a small difference under among 5g, 7g and 9g conditions. It demonstrates that a larger acceleration magnitude has insignificant effect on the temperature oscillation.

Fig. 10 depicts the temperature profiles of the loop with 25 W under configuration D for the case of the second loading mode at four different acceleration magnitude i.e. 3g, 5g, 7g and 9g. It can be seen clearly from Fig. 10 that the loop temperature presents a sharp decline after a rapid rise during the initial period of the test. After the DCCLHP starts up, the loop shows much larger temperature oscillation with the increase of the acceleration magnitude. For the heat load of 25 W, the temperature of one loop component is very close to that of the other component at 5g, 7g and 9g.

In Fig. 10(a), the evaporator temperature continues to increase after the heat load is applied. But the RTD4 temperature falls. The RTD12 temperature increases along with the CCs temperature. This indicates that the reverse flow in the loop occurs due to the effect of the acceleration. The vapor-liquid distribution in the loop changes as the acceleration is applied. The vapor with higher temperature in the evaporator reversely flows into the liquid line through the bayonet. Consequently, the RTD12 temperature increases to the maximum value of 31.8 °C. When the liquid with higher temperature gets to the RTD11 point and the RTD10 point, the temperature of the RTD11 and RTD10 increases accordingly. The decrease of the RTD4 temperature indicates that the cool fluid enters into the vapor line from the condenser. Once the evaporator temperature is increased to 33.4 °C, the vapor generates and moves into the vapor line. Therefore, the RTD4 temperature starts to increase from the minimum value of 21.8 °C. Then the vapor enters into the condenser and pushes the cooler fluid into the liquid line. As a result, the temperature of the liquid line drops sharply. The positive circulation is thus formed. The evaporator temperature gradually decreases to 25.9 °C. Finally, the DCCLHP reaches a steady state.

For the cases of 5g, 7g and 9g, the temperature of the loop shows a similar variation before the DCCLHP starts up. As can be seen in Fig. 10(b), the temperature at the inlet of the liquid line starts to increase and oscillate periodically at about 730 s. The RTD11 and RTD12 temperatures also increase and oscillate periodically. The temperature of the evaporator and CCs drops and oscillates slightly. The amplitude of the RTD10 temperature with 0.2 °C is the largest, whereas the amplitude of the RTD1 temperature is the smallest. Moreover, the temperature of the entire loop ranges from 22.6 °C to 23.3 °C.

In Fig. 10(c), when the heat and acceleration load are applied, the temperature change of the RTD4 is different with that in Figs. 10(a) and (b). It can be deduced that the effect of the acceleration results in the RTD4 temperature increase. The additional pressure head of the external loop resulted from the acceleration force exceeds the capillary force generated by the wick. As a consequence, the liquid in the vapor grooves is pushed into the vapor line. Thus, the RTD4 temperature increases. At the same time, the pressure in the evaporator core and CCs increases by the additional pressure head. It will push the vapor to reversely flow into the liquid line and further enter into the condenser. Therefore, the temperature of RTD12, RTD11, RTD10 increases in turn and the RTD4 temperature falls. Until the positive circulation is formed, the loop temperature drops rapidly. The inlet temperature of the liquid line starts to increase sharply at about 405 s and oscillate periodically. Its amplitude and period is approximate 0.2 °C and 42 s. The temperature of the entire loop ranges from 22.6 °C to 23.7 °C.

For the case of 9 g, as shown in Fig. 10(d), the variation of the temperature is similar with that shown in Fig. 10(c). After the DCCLHP starts up, it starts to oscillate in a shorter time compared to the other cases. The amplitude and period of the RTD10 temperature are 0.3 °C and 66 s, respectively. The temperature of the entire loop changes within about 1.0 °C.

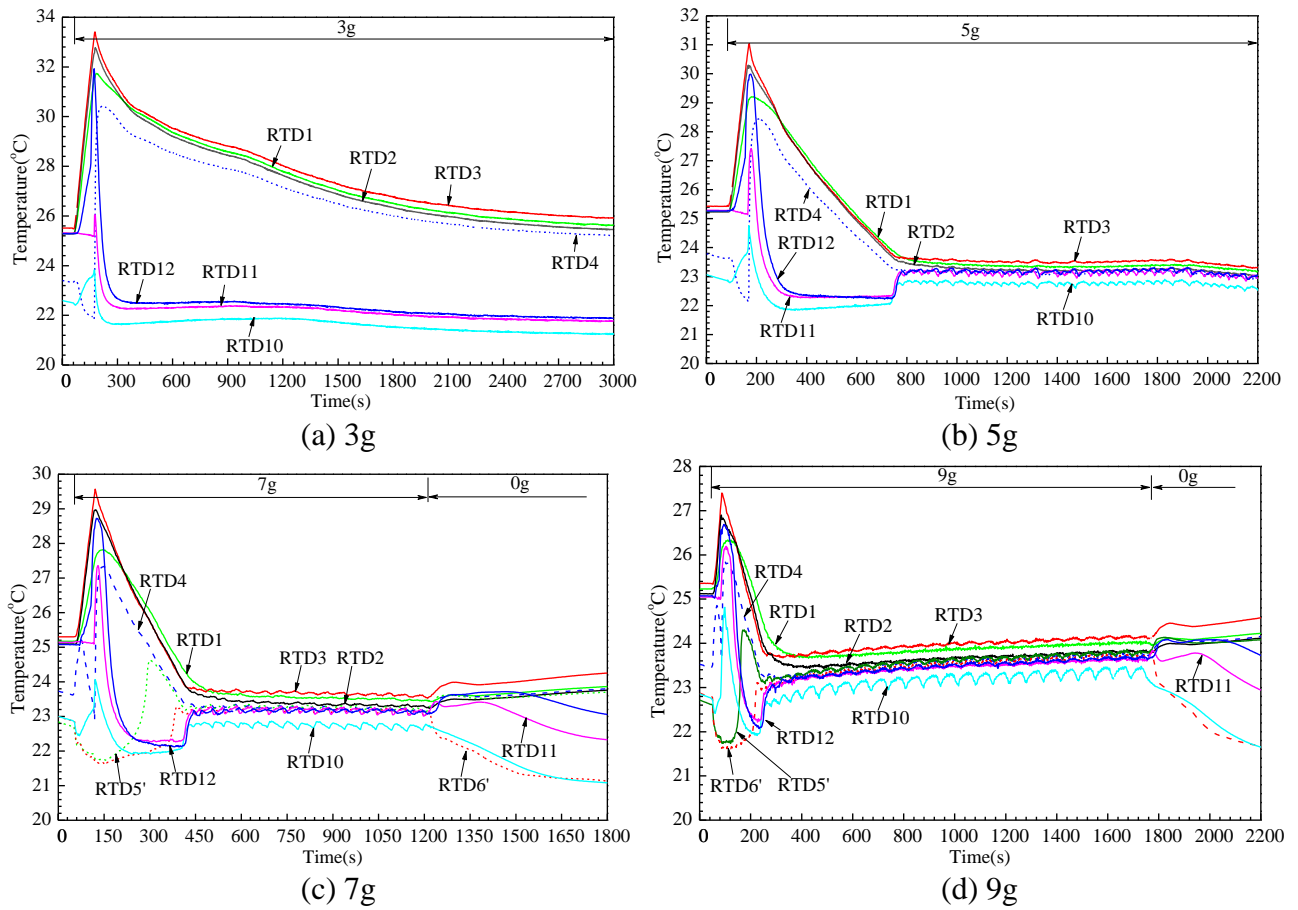


**Fig. 10.** Temperature evolutions of the loop with 25 W at 3g, 5g, 7g, 9g under configuration D and second loading mode

After the DCCLHP starts up, as demonstrated in Fig. 10(c) and (d), since the acceleration force promotes the liquid returning to the CCs, the capillary pressure difference decreases to balance the total loop pressure drop. In addition, more liquid in the CCs and evaporator core can reduce the heat leak from evaporator to CCs. Therefore, the operating temperature decreases. The loop pressure equilibrium does not reach if the capillary pressure difference reduces to 0 Pa. The acceleration force would drive the working fluid circulating in the loop. Consequently, a two-phase flow occurs in the vapor line and both the vapor and the liquid are saturated. It could be concluded that the RTD4, RTD5' and RTD6' temperatures are almost equal. After the acceleration force is stopped, the vapor-liquid distribution in the loop is also recovered to the state in gravity. A part of liquid in the CCs is displaced into the condenser which could lead to the heat leak from evaporator to CCs increase. Moreover, the capillary pressure difference is needed to drive the working fluid circulating. Therefore, the temperature difference between evaporator and CCs increases, and the evaporator temperature increases. Consequently, the temperature of the RTD4 increases. According to the temperature of RTD5' and RTD6', the vapor-liquid interface locates somewhere between both points. As a result, there is a subcooling zone in the condenser. The temperature of the liquid line drops in turn.

## CONCLUSIONS

In the current study, an experimental investigation was carried out to investigate the temperature oscillation of an ammonia-stainless steel DCCLHP with a bayonet under both terrestrial gravity and acceleration conditions. The impact of several control parameters such as different loading modes,

heat loads, acceleration directions and magnitudes on the loop temperature oscillation was analyzed and discussed. The main conclusions achieved from the current work can be concluded as follows:

(1) Temperature oscillation of the loop normally occurs at relatively high heat load of 250 W and 300 W, whereas it happens at lower heat load of 25 W and 80 W for the second loading mode. For the first loading mode at 7g, the loop temperature under configuration A and B does not oscillate at 150 W, 200 W and 250 W. Especially under configuration B, the oscillation can be weakened by the acceleration effect. The loop temperature does not oscillate at 200 W under configuration C and D. For the second loading mode at 5g, the temperature oscillation happens under configuration A, C and D for almost all heat loads.

(2) For both loading modes, the loop temperature always changes during the initial period of the acceleration. At the end of test, the temperature oscillation appears primarily on the liquid line with the first loading mode. While periodic temperature oscillation obviously occurs on the entire loop at the second loading mode.

(3) The amplitude of the liquid line is larger than that of the evaporator and CCs. But the period of these components is almost identical. The phase difference of the evaporator and the liquid line is nearly 180 degrees. For the case of 300 W and second loading mode under configuration C, the amplitude of evaporator at 3g, 5g, 7g and 9g is 0.6 °C, 0.3 °C, 0.2 °C and 0.3 °C. The period is 66 s, 36 s, 34 s and 36 s, respectively.

(4) The acceleration effect alters the vapor-liquid distribution and the pressure drop of the external loop, and further changes the heat leak from the evaporator to the CCs. Two-phase flow instability in the condenser could be strengthened or weakened by the acceleration effect. Temperature oscillation could be introduced by the combination of the above factors.

#### ACKNOWLEDGMENT

The authors acknowledge the financial supports from the Fundamental Research Funds from China Academy of Space Technology (BISEE2019-009) and Science Foundation for Distinguished Young Scholars (2020-JCJQ-ZQ-042).

#### REFERENCES

- [1] X Y You, J H Liu, N Hua, et al. Experimental study on flow boiling of refrigerant R1233zd (E) in microchannels: Heat transfer. *Applied Thermal Engineering*, 2021, 182: 116083.
- [2] M Levêque, S Dutour, J Lluc, et al. Experimental study of a Capillary Pumped Loop assisted with a mechanical pump placed at the evaporator inlet. *Applied Thermal Engineering*, 2020, 169: 114850.
- [3] J Li, G Zhou, T Tian, et al. A new cooling strategy for edge computing servers using compact looped heat pipe. *Applied Thermal Engineering*, 2021: 116599.
- [4] L Bai, Y Tao, Y Guo, G Lin. Startup characteristics of a dual compensation chamber loop heat pipe with an extended bayonet tube. *International Journal of Heat and Mass Transfer*, 2020, 148: 119066.
- [5] B Siedel, V Sartre, F Lefèvre. Literature review: Steady-state modelling of loop heat pipes. *Applied Thermal Engineering*, 2015, 75: 709-723.
- [6] Y F Maydanik, S V Vershinin, M A Chernysheva. Investigation of thermal characteristics of a loop heat pipe in a wide range of external conditions. *International Journal of Heat and Mass Transfer*, 2020, 147: 118967.
- [7] K A Goncharov, E Y Kotlyarov, F Y Smirnov, et al. Investigation of temperature fluctuations in loop heat pipes. *SAE Technical Paper No.941579*, 1994.
- [8] J Ku, L Ottenstein, M Kobel, et al. Temperature oscillations in loop heat pipe operation. *AIP Conference Proceeding*. 552: 255-262, 2001.

- [9] J Ku, J I Rodriguez. Low frequency high amplitude temperature oscillations in loop heat pipe operation. SAE Technical Paper No.2003-01-2386, 2003.
- [10] J Ku. High frequency low amplitude temperature oscillations in loop heat pipe operation. SAE Technical Paper No.2003-01-2387, 2003.
- [11] Y Chen, M Groll, R Mertz, et al. Steady-state and transient performance of a miniature loop heat pipe. International Conference on Nanochannels, Microchannels, and Minichannels. 2005, 41855: 183-189.
- [12] S Launay, V Platel, S Dutour, et al. Transient modeling of loop heat pipes for the oscillating behavior study. Journal of Thermophysics and Heat Transfer, 2007, 21(3): 487-495.
- [13] T T Hoang, R W Baldauff. A Theory for Temperature opscillations in loop heat pipes. 42nd International Conference on Environmental Systems 15-19 July 2012, San Diego, California. AIAA 2012-3478.
- [14] X F Zhang, J P Huo, S F Wang. Experimental investigation on temperature oscillation in a miniature loop heat pipe with flat evaporator. Experimental Thermal and Fluid Science, 37: 29-36, 2012.
- [15] J T Feng, G P Lin, L Z Bai. Experimental investigation on operating instability of a dual compensation chamber loop heat pipe. Science in China Series E: Technological Sciences, 2009, 52(8): 2316-2322.
- [16] G P Lin, N Li, L Z Bai, et al. Experimental investigation of a dual compensation chamber loop heat pipe. International Journal of Heat and Mass Transfer, 2010, 53: 3231-3240
- [17] T Adachi, K Fujita, H Nagai. Numerical study of temperature oscillation in loop heat pipe. Applied Thermal Engineering, 2019, 163: 114281.
- [18] Q Zhang, G Lin, X Shen, et al. Visualization study on the heat and mass transfer in the evaporator compensation chamber of a loop heat pipe. Applied Thermal Engineering, 2020, 164: 114472.
- [19] D Gai. Temperature oscillation mechanism of a flat-type loop heat pipe. Heat Transfer Research, 2020, 51(14): 1301-1315.
- [20] X Li, B Xu, G Zhang, et al. Experimental investigation on the impact of pressure head of evaporation during the loop heat pipe operation. Applied Thermal Engineering, 2021, 185 (25): 116455.
- [21] S He, P Zhou, Z Ma, et al. Experimental study on transient performance of the loop heat pipe with a pouring porous wick. Applied Thermal Engineering. 2020, 164: 114450.
- [22] J Xu, D Wang, Z Hu, et al. Effect of the working fluid transportation in the cooper composite wick on the evaporation efficiency of a flat loop heat pipe. Applied Thermal Engineering. 2020, 178: 115515.
- [23] J Ku, L Ottenstein, T Kaya, et al. Testing of a loop heat pipe subjected to variable accelerating forces, Part 2: Temperature stability. SAE Technical Paper, No. 2000-01-2489, 2000.
- [24] A J Fleming, S K Thomas, K L Yerkes. Titanium-water loop heat pipe operating characteristics under standard and elevated acceleration fields. Journal of Thermophysics and Heat Transfer, 2010, 24(1): 184.
- [25] K L Yerkes, J D Scofield, D L Courson, et al. Steady-periodic acceleration effects on the performance of a loop heat pipe. Journal of Thermophysics and Heat Transfer, 2014, 28(3): 440-454.
- [26] Y Q Xie, Y Zhou, D S Wen, et al. Experimental investigation on transient characteristics of a dual compensation chamber loop heat pipe subjected to acceleration forces. Applied Thermal Engineering, 2018, 130: 169-184.
- [27] Y Q Xie, X Y Li, L Z Han, et al. Experimental study on operating characteristics of a dual compensation chamber loop heat pipe in periodic acceleration fields. Applied Thermal Engineering, 2020: 115419.
- [28] Y Q Xie, X Y Li, S J Dong, et al. Experimental investigation on operating behaviors of loop heat pipe with thermoelectric cooler under acceleration conditions. Chinese Journal of Aeronautics, 2020, 33(3): 852-860.